Biochimica et Biophysica Acta 815 (1985) 159–169
Elsevier

BBA 72564

Membrane glycoprotein and surface free energy changes in hypoxic fibroblast cells

S.A. Johnstone [a], S. Schurch [b], D.J.L. McIver [c], E.A. Jacobson [a] and E.R. Tustanoff [a,d,*]

Department of [a] Biochemistry, [b] Biophysics and [c] Pharmacology, University of Western Ontario and [d] Department of Clinical Pathology, Victoria Hospital, London, Ontario N6A 4G5 (Canada)

(Received October 5th, 1984)

Key words: Glycoprotein; Cell surface; Surface free energy; Contact angle; Scanning electron microscopy; Hypoxia; (Chinese hamster lung fibroblast)

Hypoxia affects the biochemistry of mammalian cells and thus alters their sensitivity to subsequent chemo- and radiotherapy. When V79 Chinese hamster lung fibroblasts were grown under conditions of extreme hypoxia (< 10 ppm O_2) there was a significant shift in the membrane glycoprotein composition. Scanning electron microscopy revealed altered cell surface morphology including loss of pseudopodial projections. Experiments to determine changes in interfacial free energy of these cells using equilibrium two phase systems of poly(ethylene glycol) (PEG) and dextran were carried out. Test fluid droplets of the denser dextran-rich phase were formed on layers of cells in the PEG-rich phase as the bathing medium, and the contact angles the droplets made with the cell layers were measured from photomicrographs. The contact angles on cells in the plateau phase increased significantly with time of exposure to hypoxia, from 25° (zero time) to 35° (6 h) to 60° (9 h). Contact angles on cells in the exponential phase increased from 80° (zero time) to 150° after 20 h of hypoxia. It appears that the altered contact angles reflect changes in cell surface hydrophobicity that may, in part, reflect alterations in the membrane glycoprotein composition.

Introduction

In solid tumor masses a substantial number of hypoxic cells arises as a result of the outgrowth of tumor cells in proportion to their blood supply. The relative radio- and chemotherapeutic resistance of hypoxic cells may be responsible for the failure of a number of different cancer therapy modalities. Successful treatment with any therapeutic agent depends on exploiting the principle of selective toxicity i.e. affecting cancer rather than host cells. Selective toxicity in turn, depends on functional differences between these two cell populations whch may be exploited by identifying changes in their biochemical/or and biophysical properties.

Biochemical changes in hypoxic cells include alterations in both protein and lipid metabolism. Several workers have detected decreased protein synthesis in hypoxic cells [1,2]. Li and Shrieve [1] showed that hypoxically cultured Chinese hamster ovary fibroblasts manifested decreased rates of incorporation of labelled precursors into proteins and that these cells on restoration to an oxygen environment were characterized with induced 'shock' proteins [1,3]. In real ischemia, incorporation of [^{3}H]leucine was decreased more than 70% in kidney tissue homogenates and brush-border fractions after 25 min of ischemia; in contrast, on

* To whom correspondence should be addressed.

oxygen recovery a burst in protein synthesis was observed [1,4].

Under hypoxic conditions lipid metabolism is markedly altered. Adebonojo et al. [5] and Jacobson [6] noted the early accumulation of lipid droplets when cells were grown under hypoxic tissue culture conditions. In V79 Chinese hamster lung fibroblasts, electron microscopic examination showed the accumulation of homogeneous cytoplasmic droplets that dissipated when the cultures were returned to an aerobic environment. Gordon and his co-workers [7] suggested that the lipid accumulation was due to an inability of the cells to oxidize fatty acids and not due to autophagic processes. These workers also found an increase in the lipid/protein ratio in mouse fibroblasts grown in cell cultures exposed to limiting oxygen tensions (3×10 ppm O_2) for 48 h.

While the biochemical analyses described above have been performed on whole cells, there is considerable interest in the cell surface in both physiological and pathological states. Hypoxia has been shown to alter several functional properties of the cell membrane, including ion permeability, enzyme activity, lipid composition and fluidity and membrane morphology [8–10]. Ultimately, all cell-environment interactions must involve events at the cell surface. Such interactions may include: physiological processes such as cell adhesion; pathological processes such as malignant transformation; laboratory manipulations during cell separation and therapeutic applications such as selective drug delivery. Morphology, analytic biochemistry and biophysics are all used to characterise the cell surface; each approach has its strengths and weaknesses and we do not yet understand the detailed relationships between the information yielded by these more or less distinct disciplines. Investigations to date have indicated that a biophysical property of the cell surface, the interfacial free energy (a defined equilibrium thermodynamic potential) may provide a useful predictive criterion of cell surface interactions [11,12] and that this property may be correlated with both the lipid and glycoprotein composition of the cell surface [13]. Improving our knowledge of the uses and limitations of this approach requires the simultaneous assessment of all three cell surface properties (morphology, composition and thermodynamics) under well controlled conditions of physiological or pathological interest.

In the work presented here we have examined the surface morphology of hypoxic cells and have determined the glycoprotein composition of plasma membranes isolated from these cells. The physical effects of these surface alterations have been investigated by direct measurements of cell-medium interfacial free energy, using phase separated aqueous solutions. The results indicate that hypoxia affects both the biochemical and biophysical properties of the cell surface, and may have implications for both the isolated and chemotherapy of hypoxic cancer cells.

Materials and Methods

Culture of cells

V79 Chinese hamster lung fibroblasts were cultured in Eagle's basal medium (Gibco Canada, Burlington, Ontario) containing Hanks salts (pH 7.4) supplemented with 2 mM L-glutamine, 100 IU/ml penicillin and 100 mg/ml streptomycin and supplemented with 13% fetal calf serum. Cultures were maintained at 37°C in a humidified atmosphere of 97% air/3% CO_2.

Hypoxia

Cells (125 000 per plate) were seeded on 60×15 mm glass petri dishes containing 3 ml of culture medium. Exponential cultures were used on day 2, plateau phase cultures were maintained for 8 days, feeding daily with fresh media starting day 3. To generate extreme hypoxia plates were sealed in air-tight aluminum chambers which were successively evacuated and gassed at 0°C with a 95% nitrogen/5% CO_2 mixture until an oxygen tension of less then 10 ppm was achieved [14]. Once equilibration was obtained, the chambers were placed in a circulating water bath at 37°C to initiate hypoxic growth. Control cultures were made hypoxic in a similar manner and then immediately returned to an aerobic environment.

Membrane preparation

At the end of the experimental incubation period (hypoxic and aerobic) the gas exchange chambers were cooled to 0°C in ice for 20 min, opened and the plates then were placed on ice.

After the medium was aspirated from the plates, the cells were scraped into phosphate-buffered saline (pH 7.4) and centrifuged ($500 \times g$). The pellet was washed three times in cold phosphate-buffered saline then resuspended in homogenization buffer (10% sucrose in phosphate-buffered saline containing 3 μg DNAase, 0.005 mM phenylmethylsulfonylfluoride, 0.02% sodium azide and 1 mM dithiothreitol and the cells were disrupted using 20–25 strokes in a Dounce homogenizer as described by Maeda et al. [15]. The extent of vesicle formation was monitored using reversed phase-contrast microscopy. Whole cells and nuclei were removed by centrifugation ($500 \times g$, 20 min) and the enriched membrane fraction was concentrated by further centrifugation ($8000 \times g$, 20 min). The $8000 \times g$ pellet was resuspended in homogenizing buffer and layered over a solution of 41% sucrose in phosphate-buffered saline. Membrane fraction was collected at the interface after centrifugation ($95\,000 \times g$, 1 h, Beckman SW 27.1 rotor). The plasma-enriched fraction was diluted to 20 ml with homogenizing buffer and pelleted at $95\,000 \times g$ for 30 min. Samples from these pellets were fixed in glutaraldehyde and processed as previously described for electron microscopy [6]. Protein was determined by a modified Lowry assay [16]. Membrane protein fractions to be used for polyacrylamide gel electrophoresis were suspended in a solution containing 0.065 M Tris-HCl buffer (pH 6.8), 2% SDS, 10% glycerol, 5% 2-mercaptoethanol solution and stored frozen until used.

SDS-polyacrylamide protein electrophoresis and lectin labelling of glycoproteins were carried out using a procedure described by Cates et al. [17]. The gels were fixed in 58% methanol, penetrated with binding buffer and then labelled with ^{125}I-concanavalin A (CalBiochem-Behring Co., Los Angeles, CA) overnight. The labelled gels were washed with buffer and fixed in a solution containing 25% isopropanol, 10% acetic acid and 0.03% Coomassie blue. Autoradiograms of the gels were carried out as described by Burridge [18,19] and after developing were scanned by densitometry (Model 1705, Artionex Inc., St. Louis, MO) and quantitated using an Artionex PC-12 Computer.

For scanning electron microscopy (SEM) cells were cultured on sterile glass slips in the same manner as described above. To prepare the cells for SEM the slides on which the cells had grown were washed three times in phosphate-buffered saline, once in double distilled water, then placed in half-strength Karnowsky's fixative [20]. The fixed cells were dehydrated through a series of alcohol rinses followed by acetone, and then subjected to critical point drying. The slides were attached to scanning electron microscope stubs with silver electrical contact paint then spater coated with gold-palladium using a Technic spatterer [20]. Fixed cells were viewed using a Hitachi S560 scanning electron microscope.

Measurement of surface free energies

An aqueous two phase polymer system of 4% (w/w) poly(ethylene glycol) (mol. wt. 20 000) and 4% (w/w) dextran (mol. wt. 500 000) in 10 mM Hepes buffered Ringer's solution, pH 7.3 was used [12]. Exponential V79 cells grown under aerobic and extremely hypoxic conditions as described above were scraped from the plates and resuspended in the PEG-rich upper phase of the 2-phase system. The cells were then centrifuged onto cellulose acetate membranes (pore diameter 0.45 μm, Millipore Corp., Montreal, Canada). The filters were then immersed in the PEG-rich phase at

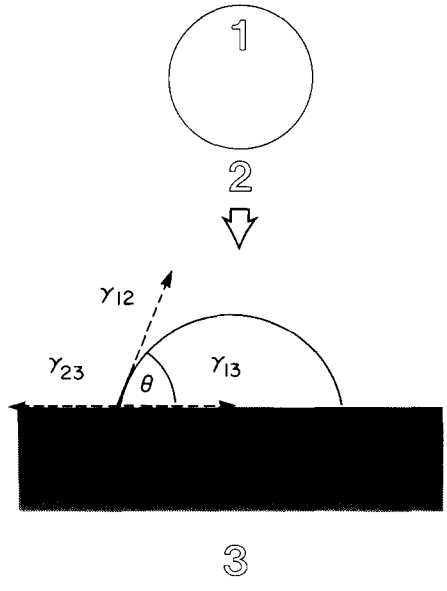

Fig. 1. Relationships between the interfacial free energies, and the contact angle at a 3-phase boundary. Phase 1, dextran phase (γ_1); phase 2, PEG (γ_2); phase 3, cell surface (γ_3).

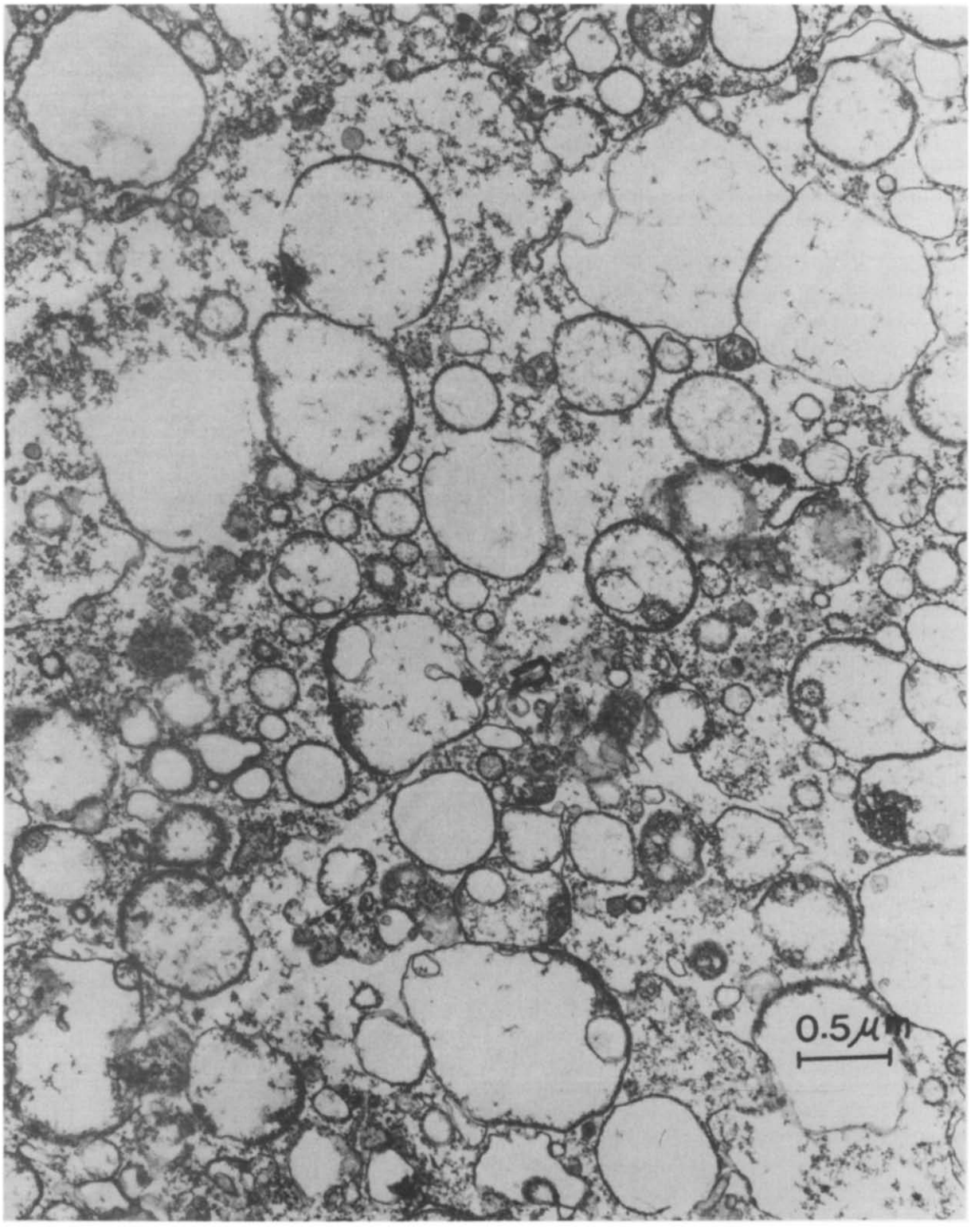

Fig. 2. Electron micrograph of a plasma membrane-enriched cell fraction from hypoxic cells. V79 fibroblast cells were grown for 9 h under extreme hypoxic conditions (<10 ppm O_2). The plasma membrane-enriched fraction was prepared as described in Methods and subsequently fixed for electron microscopy.

room temperature in a chamber with optically flat glass windows as previously described [12]. Plateau phase cells were grown on glass cover slips and supplemented with fresh standard medium daily until a complete monolayer was formed. The hypoxic cells were cultured as described above. The monolayer cells on the glass cover slips were placed in a microscope chamber, the cell layers covered with the PEG-rich phase as previously described [12] and a series of dextran-rich droplets (approx. 0.1 mm diameter) were placed on the cell layers. After 10 to 15 min, the contact angles were measured with a Nikon SMZ microscope equipped with a protractor eye-piece (Nikon Co., Tokyo, Japan). The angle was taken as the final advancing contact angle. Between 20 and 40 contact angles were measured per sample. The interfacial tension between the dextran-rich phase and the PEG-rich

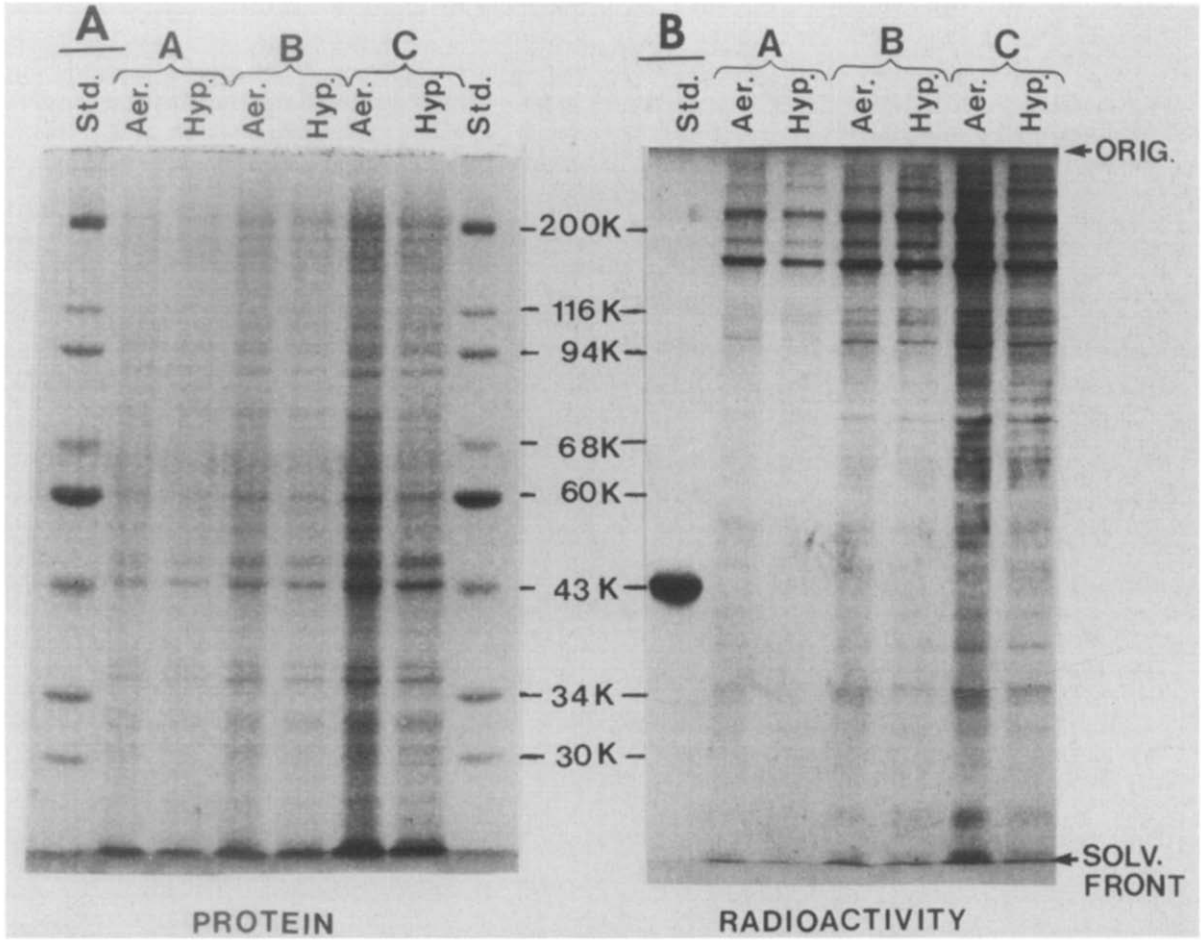

Fig. 3. Glycoprotein polyacrylamide gel electrophoresis of a plasma membrane-enriched fraction obtained from hypoxic cells. V79 fibroblast cells were grown in air ($2.1 \cdot 10^5$ ppm O_2) or under extreme hypoxic (<10 ppm O_2) for 9 hours. The plasma membrane-enriched cell fractions were isolated by gradient centrifugation and the protein components separated by polyacrylamide gel electrophoresis. The resulting chromatogram was stained with Coomassie blue for protein (Chromatogram A), then labelled with ^{125}I-concanavalin A as described in Methods and exposed to a photographic film for 8 days. Chromatogram B is a photograph of the radiogram of the glycoprotein labelled from the plasma membrane enriched protein fractions. Appropriate protein and glycoprotein standards of known molecular weights were run as markers and are identified as their average molecular weight ($\times 10^{-3}$). Lanes A, B and C represent 100, 200 and 500 μl of the membrane preparation applied to the chromatogram and Aer. and Hyp. designate samples from aerobic and hypoxic cells, respectively.

phase of the 2-phase polymer system was determined from the analysis of the shapes of sessile drops as previously described [13].

Studies of interfacial tensions in colloid liquid/vapor systems usually take as their starting point the equation derived by Young in 1805:

$$\gamma_{1,3} = \gamma_{2,3} + \gamma_{1,2} \cos \theta \quad (1)$$

where θ is the angle of contact a fluid drop makes at the surface, γ is the interfacial tension, and the subscripts 1, 2 and 3 denote the vapor, liquid and solid phases (Fig. 1). In our test system, 1 denotes the PEG-rich phase and 2 the dextran-rich phase of the 2-phase system, while 3 is the layer of cells, immersed in the PEG-rich phase.

From Fig. 1 the free energy of adhesion of the cell surface to the dextran-PEG interface (ΔF_{adh}) is expressed as:

$$\Delta F_{adh} = \gamma_{1,2}(1 + \cos \theta) \quad (2)$$

Differences in the free energies of adhesion between two states correspond to differences in the chemical affinity between the surfaces.

Results

The imposition of anaerobic growth conditions on V79 fibroblast cells altered their overall protein metabolism. After 9 h of exposure to extreme hypoxia, the protein content of these cells decreased from 0.32 ± 0.04 mg/10^6 cells to $0.27 \pm 0.03/10^6$ cells. When attention was focused on the protein profiles of isolated plasma membranes of these cells marked changes were noted. The isolated fractions appeared to be relatively clean preparations by electron microscopic (cf. Fig. 2) and enzyme marker criteria. The $(Na^+ + K^+)$-ATPase activity of membranes from aerobic cells was enriched 10-fold (0.69 μg P_i liberated/mg protein per h in whole cell vs. 6.05 μg P_i liberated/mg protein per h in plasma membrane-enriched cell fractions). The activity of this enzyme in plasma membrane-enriched cell fractions from hypoxic cells was not detectable. These observations are in accord with those of Godin et al. [21] who reported irreversible loss of this enzyme activity in ischemic heart preparations.

After resolving the proteins from the plasma membrane enriched fractions from both aerobic

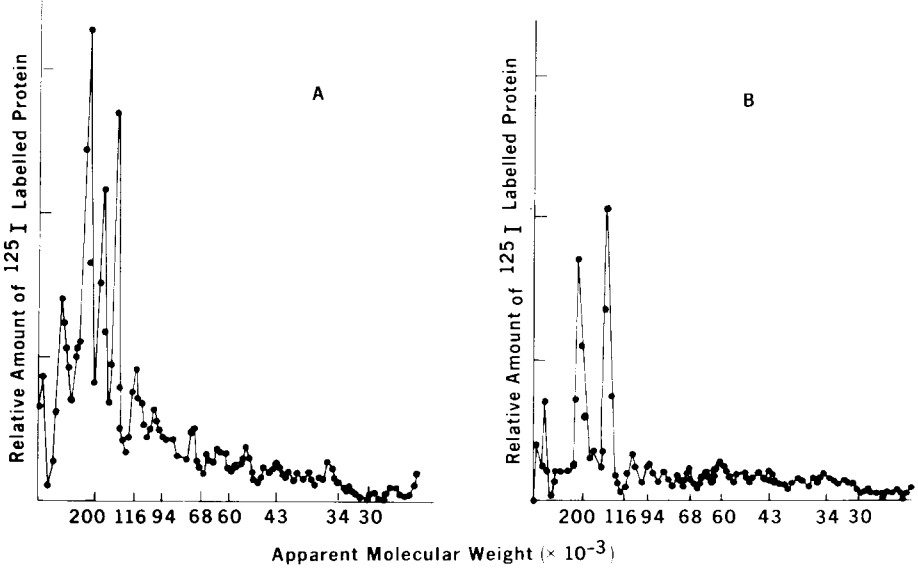

Fig. 4. Densitometry tracing of ^{125}I-concanavalin A labelled membrane glycoproteins from aerobic and hypoxic cells. The developed film from Chromatogram B Fig. 3 was scanned in a densitometer and the traces are illustrated in this figure. Scan A represents the trace of aerobic labelled membrane glycoproteins and Scan B hypoxic labelled membrane glycoproteins.

and hypoxic cells, different binding patterns were observed after polyacrylamide gel electrophoresis. The results of these experiments are illustrated in Fig. 3. Proteins with apparent molecular weights ($\times 10^{-3}$) of 92, 48 and 37 had decreased while those of 56, 55 and 30 appeared to increase during the transition of cells to a hypoxic metabolism.

Densitometer scans (Fig. 4) of the autoradiographs of these gels (cf. Fig. 3) suggest that there are elevated concentrations of glycoproteins in hypoxic membrane fractions of apparent molecular weight ($\times 10^{-3}$) of 61, 70, 36 while the labelling intensity of the other bands have decreased. The glycoprotein bands at 221 000, 160 000 and 113 000 seen in aerobic cells are considerably decreased in the gels of hypoxic membranes.

Figs. 5–7 show scanning electron micrographs of the surface of hypoxic and aerobic fibroblast cells and it can clearly be seen there are marked differences in their surface topology. Aerobic cells (Fig. 5) are characterized by their external surfaces being covered with many closely packed microvilli. After 9 h of exposure to hypoxic marked surface restructuring was observed in the V79 cells (Fig. 6). Overall the cells were rounded and had lost their characteristic fibroblast shape. The microvilli disappeared and were replaced by long spike-like projections. On higher magnification, the surface appeared globular in nature, with deep invaginations having a bark-like surface. After 24 h of

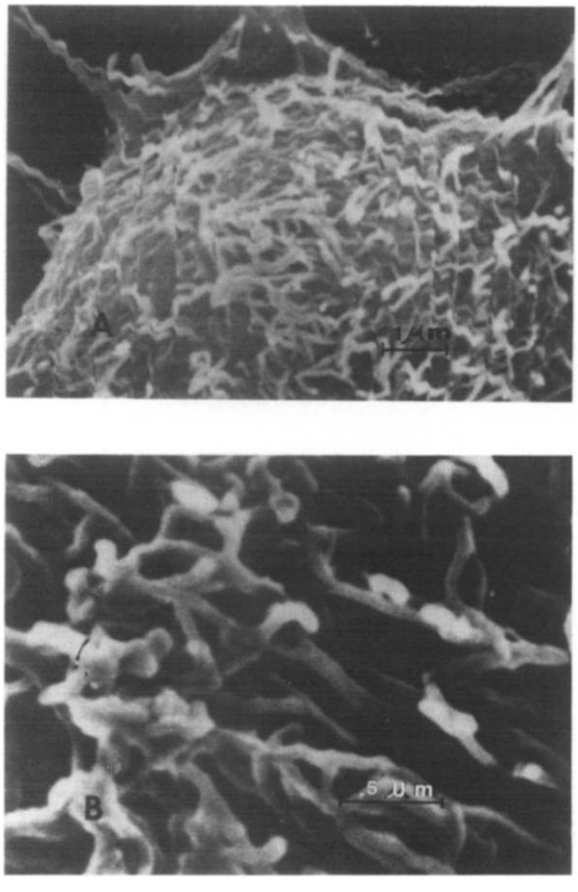

Fig. 5. Scanning electron micrographs of cells grown in air for 9 h. V79 fibroblast cells were grown under aerobic conditions ($2.1 \cdot 10^5$ ppm O_2). Cells were prepared for scanning electron microscopy as described in Methods. Plates A and B represent two fields at different magnification.

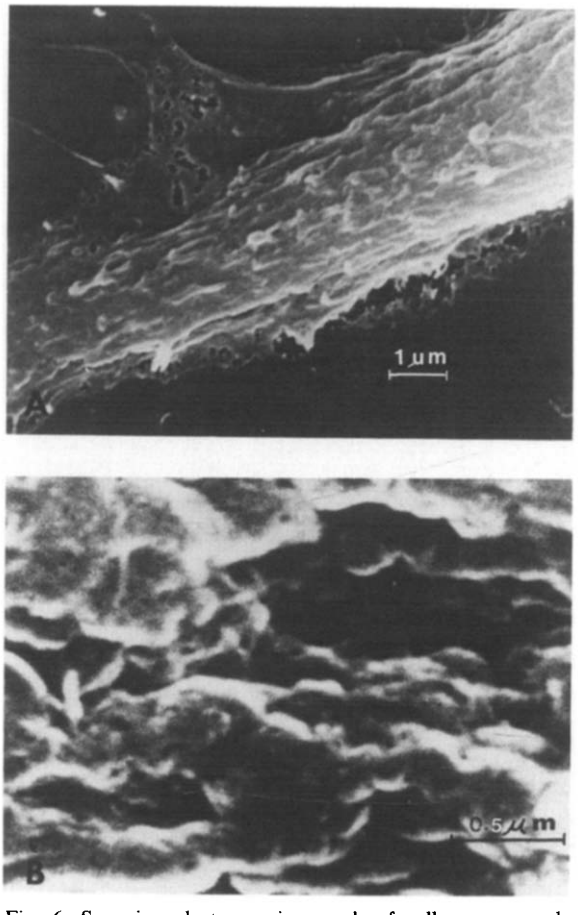

Fig. 6. Scanning electron micrograph of cells grown under extreme hypoxic conditions for 9 h. Conditions were identical to those described in the legend to Fig. 5.

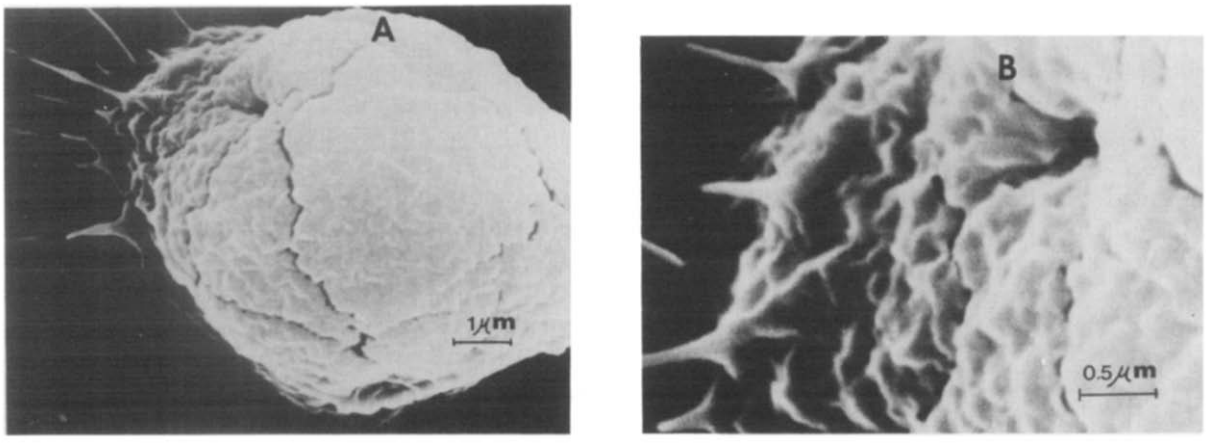

Fig. 7. Scanning electron micrograph of cells grown under extreme hypoxic conditions for 24 h. Conditions were identical to those described in the legend to Fig. 5.

oxygen deprivation further topographic changes were noted (Fig. 7). The cells were elongated and often terminated in knob-like structures. The surface of the cell was highly ruffled giving the appearance of layered sheets with occasional blebs. Emanating from these surfaces, particularly in the axial surface were long narrow spikes. The membrane surface also had deep invaginations. At low magnification (not shown) the cells appeared to be lifting off from the glass surface, indicating loss of contact with their growing surface. It is apparent that cellular oxygen tension profoundly affects the cell's surface architecture.

Measurements of interfacial free energy showed marked differences between control and hypoxic cells. The contact angles (cf. Fig. 8 and Table I) on

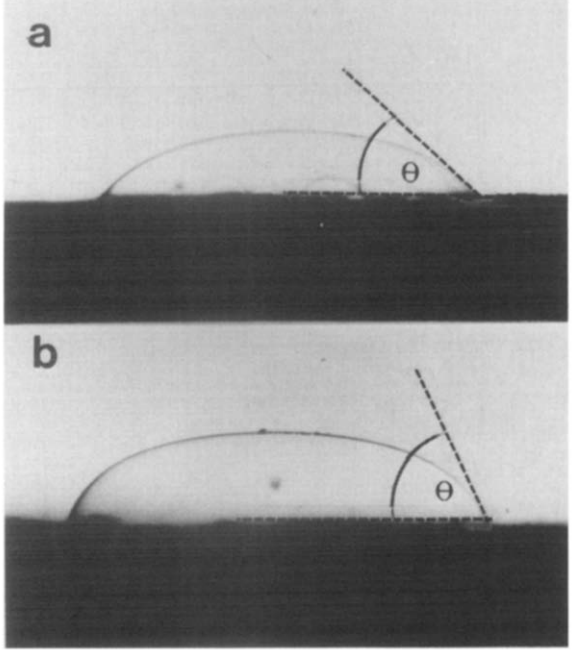

Fig. 8. Comparison of contact angles formed by a droplet of the dextran-rich phase from a dextran (4%) w/w system on layers of V79 cells grown under (a) aerobic and (b) extreme hypoxic conditions as described in Methods.

TABLE I

EFFECT OF OXYGEN TENSION ON THE MEASURED CONTACT ANGLES ON V79 CELLS

Cells were grown as plateau cultures on glass cover slips on glass plates as described in Methods until a tight monolayer of cells was formed. The growth of exponential cells, the production of extreme hypoxia and the measurement of the contact angles of the fibroblast cells were carried out as described in Methods. Each experimental growth condition was repeated three times. The results reported in this table represent the mean ± standard error of the mean (S.E.) of between 20 and 40 contact angle measurements of each of the three experiments.

	Time (h)	Oxygen tension (ppm)	Contact angle (θ) (mean ± S.E.)
Plateau cells	0	$2.1 \cdot 10^5$	25° ± 1
	6	< 10	41° ± 1
	7	< 10	44° ± 1
	9	< 10	63° ± 1
Exponential cells	20	$2.1 \cdot 10^5$	81° ± 2
	10	< 10	93° ± 2
	20	< 10	104° ± 2

the membranes of fibroblast cells grown in plateau phase cultures increased significantly with time of exposure to extreme hypoxia from 25° (zero time) progressively to 63° (after 9 h). Contact angles of cells in exponential phase increased from 81° to 104° after 20 h of oxygen deprivation. No changes were observed in contact angles of plateau phase cells grown under moderate hypoxia ($2 \cdot 10^3$ ppm O_2) for 16 h.

Discussion

Hypoxic regions can develop in areas of tumor when the neoplastic tissue proliferates to such an extent that the vascular supply is insufficient to deliver oxygen to all cells. Hypoxic cells are an obstacle to effective cancer treatment since radiation sensitivity increases nearly 3-fold when oxygen is present during the radiation exposure. Residual malignant cells, protected from radiotherapy or chemotherapy by hypoxia, may be capable of proliferating and allowing the tumor to recur. Since rational therapy involves exploiting the difference between the unwanted cells and the host, it is necessary to be able to separate the hypoxic cells from the other cells in heterogeneous tumors in order to identify possible differences between the cell populations. In the absence of an effective separation method, the present experiments were performed on hypoxic cells maintained in tissue culture. These experiments demonstrate a number of differences between hypoxic and normoxic cells which may form the basis of future separatory and therapeutic manoeuvres.

The decrease in total protein concentration may be at least partially due to inhibition of protein synthesis previously reported to occur at the level of both transcription and translation [4]. Quantitative differences in oligomannose-labelled glycoproteins, most notably in the high molecular weight proteins, were apparent after nine hours of extreme hypoxia. The endoplasmic reticulum damage induced by hypoxia, as detected by electron microscopy [6,22] may be partially responsible for altered glycoprotein levels.

Much work has been done on the lipid changes of hypoxia and ischemia. The predominant findings are decreased phospholipid and increased free fatty acid [8]. Our biochemical analyses indicate alterations in protein components of the cell membranes after hypoxic exposure.

Scanning electron microscopy at low magnification shows loss of contact with the glass surface. At higher magnification altered surface morphology of the fibroblasts is apparent. There is a loss of microvilli projections and rounding of the cells. Trump et al. [23] showed similar bleb formations in anoxic Ehrlich ascites tumor cells. Lemasters et al. [24] working with hypoxic hepatocytes showed similar membrane changes. Paddock et al. [2] found disappearance of the renal brush border during renal ischemia and lowered incorporation of protein into the brush border. In hypoxia there are altered ion levels [22] and increased membrane permeability to calcium [8]. The cellular ionic composition is very important in maintaining the cytoskeleton [25] which in turn is associated with cell surface topography [26]. Wang and Goldberg [27] correlated altered cell morphology and surface topography (retraction of long fibroblast processes and peripheral cytoplasm, ruffling of the surface and rounding of the cells), with disruption of microfilaments in chick embryo fibroblasts infected with Rous sarcoma virus. Disruption of stress fibres, microfilaments of focal contacts [28] may cause a detachment of the cell from the culture surface. Lemasters et al. [24] showed altered surface structure in hypoxic rat liver, and compared the membrane blebs formed with those generated by treating the cells with phalloidin and cytochalasin D, agents that disrupted the cell's cytoskeleton. These authors concluded that the morphological alterations induced by hypoxia were due to cytoskeletal disruptions. Our membrane preparations did not show the blebs seen by Lemasters et al. [24] and Trump et al. [23] but may show a later manifestation of hypoxic injury, i.e. disruption of the cytoskeleton coupled with cell swelling [6,28].

The surface free energy measurements indicated that the membranes of the hypoxic cells decreased in polarity when compared with aerobic cells. The cell surfaces became less 'dextran like'. The altered cells interacted more strongly with polyether-like surfaces and less strongly with carbohydrate-like surfaces. Since dextran has a less 'hydrophobic' structure than PEG, it has become popular to identify altered cell-dextran/PEG interactions as

reflecting alterations in cell surface 'hydrophobicity'. Quantitatively, from Table I, the affinity of the plateau phase cells for the dextran-PEG interface changed by $2.456 \cdot 10^{-3}$ mJ $\cdot$ m^{-2} as a result of hypoxic exposure, while the affinity of the exponential phase cells changed by $0.398 \cdot 10^{3}$ mJ $\cdot$ m^{-2}.

The glycoprotein changes rather than lipid alterations are probably mostly responsible for the alterations in cell surface free energies detected using phase separated polymers. This conclusion is based on our observations of reconstituting membrane glycoproteins into model membranes and observing the effects on the wetting behaviour of the model surfaces. Obtaining low contact angles (90° or less) with the two phase system requires the presence of high molecular weight glycoproteins [13]. Subsequent studies in our laboratory (unpublished) have shown that varying the lipid composition of this membrane has little effect provided the glycoprotein composition remains constant. From a consideration of the phase diagram of the two phase system used in the present study [12] it can be seen that the alterations in the amount of molecular weight of the membrane glycoproteins would be expected to produce higher interfacial free energies and contact angles, which is consistent with the present observations. Similar considerations may apply to the suggested effects of cell cycle on contact angles, although we have not yet studied the influence of this parameter on membrane glycoproteins.

It is also possible that the observed changes in cell volume may have contributed to the change in surface free energy by a similar effect of cell surface polymer concentration to that discussed earlier [13]. Cell volume reflects a steady-state balance between influx and efflux of water and solutes which may be described by equations of the form:

$$J_i = L_i X_i$$

$$J_e = L_e X_e$$

where J is the volume flux, L the permeability, X the driving force and the subscripts i and e denote influx and efflux, respectively. A shrinkage is observed at the beginning of hypoxic incubation [6] and must result from J_e exceeding J_i, possibly because of an increase in potassium efflux resulting from calcium release from hypoxic mitochondria [8]. The subsequent swelling [6] is similar to that reported by a number of other workers [10] reflects the influx of sodium chloride and water as volume regulation is impaired. Provided membrane material does not phase separate to or from the bulk phase, the membrane expansion accompanying swelling may also reduce the effective surface concentration of macromolecules and contribute to the higher contact angles.

The basis for the dramatic differences in surface free energy between exponential and plateau phase cells is somewhat difficult to interpret, since it may reflect the different methods of preparing these two groups of cells for analysis. If the differences in contact angles do result from real differences in cell surface free energy, they may turn out to have considerable relevance to the surface aspects of cell growth and contact inhibition. Further investigation in this area is required.

Whatever the biochemical basis for the changes in cell surface free energy induced by hypoxia, the thermodynamic measurements are unambiguous: hypoxic cells have considerably higher interfacial free energies that their normoxic counterparts. It may be possible to exploit these changes in both the investigation and treatment of hypoxic cells in solid tumors. Thus, it may be possible to improve the separation of hypoxic cells from tumors by exploiting their different surface free energies by partition in two-phase polymer systems [29]. Similarly, the surface energy differences may conceivably allow an improvement in the selectivity of tumor chemotherapy using encapsulated drugs [30].

Acknowledgements

The authors wish to express their gratitude to Dr. Margaret Creighton and Dr. G.A. Cates for their assistance with the SEM and glycoprotein labelling experiments, respectively. This work was supported by the Medical Research Council of Canada through a grant in aid to E.R.T., S.S. and D.J.L.M.

References

1 Li, G.C. and Shrieve, D.C. (1982) Exp. Cell Res. 142, 464–468
2 Paddock, J.K., Lada, W. and Lowenstein, L.H. (1981) Am. J. Physiol. 24, F28-38
3 Guttman, S.D., Glover, C.V.C., Allis, C.D. and Gorovsky, M.A. (1980) Cell 22, 299–307
4 Alberghina, M., Ragusa, N. and Guiffride, A.M. (1981) Ital. J. Biochem. 30, 229–241
5 Adebonojo, F.O., Bensch, K.G. and King, D.W. (1961) Cancer Res. 21, 252–256
6 Jacobson, E.A. (1981) Ph.D. Thesis, University of Western Ontario, London, Canada
7 Gordon, G.B., Bareza, M.A. and Bush, M.E. (1977) Am. J. Pathol. 88, 663–678
8 Chen, K.R., Abrams, J., Serroni, A. and Martin, J.T. (1978) J. Biol. Chem. 253, 4809–4818
9 Altona, J.C. and Van der Laarse, A. (1982) Cardiovasc. Res. 16, 138–143
10 Katz, A.M. and Messineo, F.G. (1981) Circ. Res. 48, 1–16
11 Neumann, H.W., Absolom, D.R., Francis, D.W., Omenyi, S.N., Spett, J.K., Policova, Z., Thomson, C., Zingg, W. and Van Os, C.J. (1983) Ann. N.Y. Acad. Sci. 416, 276–297
12 Schurch, S., Gerson, D.F. and McIver, D.J.L. (1981) Biochim. Biophys. Acta 640, 557–571
13 McIver, D.J.L. and Schurch, J. (1982) Biochim. Biophys. Acta 691, 52–60
14 Koch, C.J., Howell, R.L. and Biaglow, J.E. (1979) Br. J. Cancer 39, 321–329
15 Maeda, T., Balakrishnan, K. and Mehdi, S.Q. (1983) Biochim. Biophys. Acta 731, 115–121
16 Markwell, M.K., Haas, S.M., Tolbort, N.E. and Bieber, L.L. (1981) in Methods in Enzymology (Lowenstein, J., ed.), Vol. 72, pp. 296–303, Academic Press, New York
17 Cates, G.A., Brickenden, A.M. and Sanwal, B.D. (1984) J. Biol. Chem. 259, 2646–2650
18 Burridge, K. (1976) Proc. Natl. Acad. Sci. USA 73, 4457–4461
19 Burridge, K. (1978) in Methods in Enzymology (Ginsburg, V., ed.), Vol. 50, pp. 54–64, Academic Press, New York
20 Trevithick, J.R., Creighton, M.D., Ross, W.M. and Stewart-De Haan, J. (1981) Can. J. Opthalmol. 16, 32–38
21 Godin, D.V., Tuchek, J.M. and Moore, M. (1980) Can. J. Biochem. 58, 777–786
22 Trump, B.F. and Laiho, K.U. (1975) Lab. Invest. 33, 706–711
23 Trump, B.F., Penttila, A. and Berezesky, I.K. (1978) Virch. Arch. B: Cell Pathol. 29, 297–307
24 Lemasters, J.J., Stemkowski, C.J. and Thurman, R.G. (1983) J. Cell Biol. 97, 778–786
25 Burridge, K. and Feramisco, J.R. (1981) Nature 294, 565–567
26 Porter, K.R., Pusk, T.T., Hsie, A.W. and Kelly, D. (1974) Cell 2, 145–162
27 Wang, U. and Goldberg, A.A. (1976) Proc. Natl. Acad. Sci. USA 73, 4065–4069
28 Birchmeir, W. (1981) Trends Biochem. Sci. 7, 234–236
29 Walter, H. (1982) in Cell Separation Methods and Applications (Pretlow, T.G. and Pretlow, T.P., eds.), pp. 261–299, Academic Press, New York
30 Poste, G. and Papahadjopoulos, D. (1979) in Liposomes in Biological Systems (Allision, A.C. and Gregoriadias, G., eds.), pp. 165–183, John Wiley, New York